

Cluster Dynamical Mean-Field Methods for d-wave Superconductors: the Role of Geometry

A. Isidori¹ and M. Capone^{2,1}

¹ Dipartimento di Fisica, Università di Roma "La Sapienza", Piazzale A. Moro 2, 00185, Rome, Italy and

² SM C, CNR-INFM and ISC-CNR, Piazzale A. Moro 2, 00185, Rome, Italy

(Dated: February 21, 2024)

We compare the accuracy of two cluster extensions of Dynamical Mean-Field Theory in describing d-wave superconductors, using as a reference model a saddle-point t-J model which can be solved exactly in the thermodynamic limit and at the same time reasonably describes the properties of high-temperature superconductors. The two methods are Cellular Dynamical Mean-Field Theory, which is based on a real-space perspective, and Dynamical Cluster Approximation, which enforces a momentum-space picture by imposing periodic boundary conditions on the cluster, as opposed to the open boundary conditions of the first method. We consider the scaling of the methods for large cluster size, but we also focus on the behavior for small clusters, such as those accessible by means of present techniques, with particular emphasis on the geometrical structure, which is definitely a relevant issue in small clusters.

PACS numbers: 71.10.Fd, 71.27.+a, 75.20.Hr, 75.10.Lp

Strongly Correlated electronic materials and the solution of the models introduced to understand their behavior are one of the main challenges of modern solid state physics. Despite the intensive activity triggered by the role of correlations in high-temperature superconductors, many questions remain unanswered. The vitality of the field is testified by the development of theoretical approaches designed precisely for these systems. Among these methods, a central role is played by Dynamical Mean-Field Theory (DMFT)¹, a non-perturbative approach which generalizes the classical mean-field theory to the quantum dynamical world. The development of DMFT has allowed for a number of successes, starting from the first unified scenario for the longstanding problem of the Mott transition, and including reliable description of the electronic properties of many correlated systems².

The idea behind DMFT is analogous to classical mean-field theory, namely the assumption that each lattice site is equivalent to any other. The difference with the static case is that, within DMFT, each lattice site has a completely non-trivial dynamics. Following the above strategy, one given site can be taken as representative of the whole system: the lattice problem is therefore mapped onto a dynamical local problem, and consequently onto a single-impurity model. The effect of all the remaining lattice sites will be described by a bath, whose frequency dependence will be determined through a self-consistency condition that enforces the equivalence between the lattice and the local problems^{1,3}. The main limitation of the standard (single-site) DMFT, as we have described it so far, is the neglect of spatial correlations. This constraint, indeed, introduces some limitations which are particularly relevant in low dimensionality, and in particular it makes it impossible to treat phases with a definite spatial ordering such as d-wave superconductivity, d-density waves, stripes, dimerized states.

A few schemes have been proposed to overcome these

limitations, re-introducing short-range correlations by replacing the single impurity model with a cluster-impurity, which contains N_c sites in a given spatial arrangement.^{4,5,6} In this manuscript we compare two alternative schemes that represent somehow opposite perspectives in their ability to describe two-dimensional correlated models and d-wave superconductivity. The Dynamical Cluster Approximation (DCA)⁴ is based on a momentum-space perspective and it replaces the single momentum-independent self-energy of DMFT with the set of self-energies associated to the lattice momenta of an N_c -site cluster. For the (cluster) impurity model, this approach requires periodic boundary conditions on the cluster. The other approach we consider, the Cellular Dynamical Mean-Field Theory (CDMFT), assumes instead a real space perspective, and it generalizes more directly the mean-field spirit of DMFT⁵. In this scheme, a given cluster is chosen, and a "local" theory for the cluster degrees of freedom is obtained through the cavity method, replacing the effect of the rest of the lattice with a self-consistent effective bath. The basic approximation is to assume that the dynamical field experienced by the cluster is Gaussian.

The properties of the two methods have been compared in several papers⁷ which focused mainly on the asymptotic behavior for large clusters, and the two methods have been used to study many properties of the two-dimensional Hubbard model like, notably, d-wave superconductivity⁸. It must be underlined that, despite the simplifications introduced by the cluster methods with respect to the full lattice problem, the cluster-impurity model remains a non-trivial many-body problem, that still requires, in practice, a numerical "solver" in order to achieve the Green's functions. Among the most popular impurity solvers we remind various Quantum Monte Carlo methods (Hirsch-Fye determinant method⁹, and the more recently introduced Continuous-Time Quantum Monte Carlo¹⁰), the exact-

diagonalization approach¹¹, the numerical renormalization group¹².

As a matter of fact, present "state of the art" calculations using accurate numerical solvers are limited to fairly small clusters^{8,13}, or, if the cluster size is increased, to relatively small coupling and/or finite temperature^{4,15}, which may not be representative of the strong-repulsion regime. Such small sizes hardly allow for an accurate size scaling to describe the thermodynamic limit. It is therefore desirable to study the performance of the different cluster methods as a function of the cluster size within some approach that allows for a solution at arbitrary values of the size. This point of view has been taken in Ref. 7, where a one-dimensional exactly solvable model has been studied using both CDMFT and DCA, allowing the comparison between the two methods.

In this work we apply a similar strategy to treat a model which describes the essential physical ingredients of the cuprates, namely their two-dimensional character, the effects of strong correlations, and, most importantly, the presence of d-wave superconductivity. This model is the t-J model treated at a saddle point level, following, e.g., Ref. 16. While this model is clearly an approximation of the full two-dimensional t-J model (which lacks an exact solution), we will consider it as our "starting model". In this way we will have an exactly solvable model, containing all the main ingredients of cuprates, that we can also solve using DCA and CDMFT approaches for any finite size of the clusters. This will allow us on one hand to study the convergence of the methods in the limit of large cluster-size, but on the other hand it will lead to a benchmark of the methods for small and intermediate clusters, such as those available in present numerical calculation and in those that can be expected in a few years. Of particular interest, in this light, are the "geometrical" aspects of the different approaches. When a phase with a given spatial structure is present in a finite cluster, we can expect different behaviors according to the way in which the ordered phase fits in the chosen cluster. This will also depend on the boundary conditions, and will mark the difference between DCA and CDMFT.

The manuscript is organized as follows: In Sec. II we present the reference model, i.e., the saddle-point t-J model. In Section. III we introduce DCA and CDMFT, and their application to our model. Sec. IV presents our results, and Sec. V contains concluding remarks.

I. MODEL AND METHOD

A. The saddle-point t-J model

In this section we briefly review the derivation of the saddle-point t-J model in order to fix the notations and the main concepts. Even if we will not attempt to solve it beyond saddle point, the starting point of our analysis

is the two-dimensional t-J model

$$H = P \sum_{\langle ij \rangle} t_{ij} \sum_{\sigma} f_i^{\sigma} f_j^{\sigma} + h.c. + \sum_i \epsilon_i \sum_{\sigma} f_i^{\sigma} f_i^{\sigma} + J \sum_{\langle ij \rangle} S_i \cdot S_j - \frac{1}{4} \sum_i n_i n_{i\#} \quad (1)$$

where $S_i = \frac{1}{2} \sum_{\sigma} f_i^{\sigma} f_i^{\sigma}$ is the local spin operator, $n_i = \sum_{\sigma} f_i^{\sigma} f_i^{\sigma}$ is the local electron density and $P = \prod_i (1 - n_i n_{i\#})$ is a projection operator which restricts the fermionic Hilbert space to the low-energy subspace of empty and singly-occupied sites; the super-exchange antiferromagnetic coupling J is given by $4t^2/U$.

We introduce slave boson fields in order to keep track of the empty sites (holes): this representation allows, in fact, to replace the constraint of zero double occupancy with the following equality constraint,

$$\sum_{\sigma} f_i^{\sigma} f_i^{\sigma} + b_i^{\dagger} b_i = 1; \quad (2)$$

where $b_i^{\dagger} b_i$ acquires the meaning of a local density of holes. Enforcing this constraint by means of a local Lagrange multiplier ϵ_i , we obtain:

$$H_{sb} = \sum_{\langle ij \rangle} t_{ij} \sum_{\sigma} f_i^{\sigma} f_j^{\sigma} b_j^{\dagger} b_i + h.c. + \sum_i \epsilon_i \sum_{\sigma} f_i^{\sigma} f_i^{\sigma} + J \sum_{\langle ij \rangle} S_i \cdot S_j - \frac{1}{4} \sum_i (1 - b_i^{\dagger} b_i)(1 - b_j^{\dagger} b_j) + \sum_i P_i \sum_{\sigma} f_i^{\sigma} f_i^{\sigma} + b_i^{\dagger} b_i - 1 : \quad (3)$$

To obtain an exactly solvable model we decouple the exchange interaction $S_i \cdot S_j$ introducing three sets of Hubbard-Stratonovich fields, which allow us to treat on the same footing both the particle-hole and particle-particle channels: the reason for this approach is given by the requirement that the SU(2) particle-hole symmetry at half-filling is being preserved.

A static mean-field approximation is then achieved by replacing the auxiliary fields and the Lagrange multiplier with their saddle-point values. Setting $h S_i = 0$ and neglecting the 4-boson hole-hole interaction, which is $O(x^2)$ near half-filling ($x = N_{\text{holes}}/N$ is the hole doping), the slave-boson mean-field Hamiltonian reads

$$H_{sb}^{MF} = \sum_{\langle ij \rangle} t_{ij} \sum_{\sigma} (f_i^{\sigma} f_j^{\sigma} b_j^{\dagger} b_i + h.c.) + \sum_i \epsilon_i \sum_{\sigma} f_i^{\sigma} f_i^{\sigma} + \sum_i \epsilon_i b_i^{\dagger} b_i + \sum_{\langle ij \rangle} (t_{ij} f_i^{\sigma} f_j^{\sigma} + h.c.) + \sum_{\langle ij \rangle} \epsilon_{ij} (f_i^{\sigma} f_{j\#}^{\sigma} - f_{i\#}^{\sigma} f_j^{\sigma}) + h.c. ; \quad (4)$$

with the particle-hole and particle-particle amplitudes given by

$$i_j = \frac{3}{8} J h f_j^y f_i i; \quad (5)$$

$$i_j = \frac{3}{8} J h f_{i\#} f_{j\#} f_{i\#} f_{j\#} i; \quad (6)$$

The last step of our approximation consists in decoupling the kinetic term of Eq. (4), and this leads to an effective hopping amplitude $t_e = t h_j^y b_{i\#} i$ for the fermionic degrees of freedom: assuming full boson condensation at $T = 0$, we can set $h_j^y b_{i\#} i = j b_{i\#} i^2 = x$ and consider, at last, $t_e = x t$. At small doping the effects of strong correlations are thus summarized in the renormalization of the free-fermion hopping term, which leads to a strong suppression of the kinetic energy, $O(xt)$, and to a relative enhancement of the super-exchange energy, $O(J)$, i.e. finite, as $x \rightarrow 0$.

In finding a self-consistent solution of the Hamiltonian (4), it has been shown¹⁷ that while at half-filling there are an infinite number of degenerate ground-states, connected together by the $SU(2)$ rotations of the particle-hole symmetry, as soon as doping breaks the $SU(2)$ invariance the lowest-energy state is found to be¹⁶ the d-wave solution $x = y = \frac{1}{2}$, $x = y = \frac{1}{2}$. We will therefore consider this kind of solution throughout our analysis.

Writing the fermionic part of H_{sb}^{MF} in Fourier space, we obtain

$$H_f = \sum_k (k) f_k^y f_k + \sum_k (f_k^y f_{k\#}^y + f_{k\#} f_k); \quad (7)$$

$$k = 2(t_e + \frac{1}{2})(\cos k_x + \cos k_y); \quad (8)$$

$$k = 2(\cos k_x - \cos k_y); \quad (9)$$

where the parameters $\frac{1}{2}$ and $\frac{1}{2}$, representing respectively a renormalization of the hopping and a d-wave order parameter, are determined by the self-consistency equations (5)(6). These in Fourier space read

$$= \frac{3}{8} J \sum_k \frac{d^2 k}{(2)^2} h f_k^y f_k i (\cos k_x + \cos k_y) \quad (10)$$

$$= \frac{3}{8} J \sum_k \frac{d^2 k}{(2)^2} \frac{(k)}{2E_k} \tanh \frac{E_k}{2} (\cos k_x + \cos k_y);$$

$$= \frac{3}{8} J \sum_k \frac{d^2 k}{(2)^2} h f_k^y f_{k\#} i (\cos k_x - \cos k_y) \quad (11)$$

$$= \frac{3}{8} J \sum_k \frac{d^2 k}{(2)^2} \frac{k}{2E_k} \tanh \frac{E_k}{2} (\cos k_x - \cos k_y);$$

where $E_k = (k)^2 + \frac{k^2}{2}$ are the eigenvalues of the Hamiltonian (7). The fermionic chemical potential is instead determined by the number equation

$$1 - x = 1 - \sum_k \frac{d^2 k}{(2)^2} \frac{(k)}{E_k} \tanh \frac{E_k}{2}; \quad (12)$$

obtained by imposing the fermion density to be $(1 - x)$.

B. Cluster Approximations

We are now in the position to compare the exact solution of the saddle-point model (4) with the approximate cluster solutions. Within cluster DMFT methods an effective action for the cluster degrees of freedom is defined as

$$S_e = \sum_d \sum_{c \in \text{cluster}} c^y (i) G^{-1}(i) c(i) + \sum_{c \in \text{cluster}} \sum_{n=1}^{\infty} U n \cdot (i) n_{\#}(i); \quad (13)$$

where G^{-1} is a dynamical "Weiss" field. By computing the cluster Green's function $G(i) = \text{tr} c(i) \partial_i$, the cluster self-energy is obtained as

$$c(i|_n) = G^{-1}(i|_n) - G^{-1}(i|_n); \quad (14)$$

The two methods differ in the way the new Weiss field is obtained through the knowledge of the cluster self-energy $c(i|_n)$.

Within CDMFT the "local" Green's function for the cluster is calculated as

$$G_{loc}^{-1}(i|_n) = \sum_{c \in \text{cluster}} \sum_{n=1}^{\infty} \frac{1}{i|_n + t_k c(i|_n)} \frac{dk}{2\pi N_c}; \quad (15)$$

where the momentum-integral extends over the reduced Brillouin zone associated to the N_c -site cluster, t_k is the Fourier transform of the cluster hopping term. $G_{loc}(i|_n)$ is then used to obtain a new Weiss field

$$(G_0^{new})^{-1}(i|_n) = c(i|_n) + G_{loc}^{-1}(i|_n); \quad (16)$$

which determines the new effective action (13) from which a new $G(i|_n)$ can be obtained: the procedure is then iterated until convergence. We stress that this method does not impose lattice translational invariance.

The spirit of DCA is instead to generalize the momentum-independence of the self-energy, characteristic of the single-site DMFT, to a small cluster. Thus one defines a coarse-grained self-energy for every reciprocal lattice momentum k_c associated to the cluster at hand. The analogue of (15), which expresses the lattice Green's function in terms of the cluster self-energy, is given by

$$G(k_c + K; i|_n) = \frac{1}{i|_n + t(k_c + K) c(k_c; i|_n)}; \quad (17)$$

while the self-consistency relation between the Weiss field and the cluster self-energy now reads

$$G_0^{-1}(k_c; i|_n) = \frac{N_c}{N} \sum_K G(k_c + K; i|_n) + c(k_c; i|_n); \quad (18)$$

In these expressions, all the cluster quantities appear as functions of the cluster momenta k_c , and the K integration over the reduced Brillouin zone is nothing but a coarse-graining of the lattice Green's function around these momenta.

A crucial observation is that the diagonal nature in momentum space of the DCA equations requires that the cluster part of our effective action has periodic boundary conditions. As we will discuss, this may represent a severe constraint, especially for small cluster sizes.

Even if DCA is naturally defined in momentum space, it is useful to recover a real-space formulation also for this cluster approach, in order to have a unified formalism which makes easier the comparison between the two methods. Performing a Fourier transform upon the cluster momenta, all the cluster quantities $Q(k_c)$ become cyclic matrices in the real-space cluster indexes, i.e., with the matrix elements Q_{ij} depending only on $(i-j) \bmod L_c$: this means that translational invariance is preserved within the cluster, which thus must have periodic boundary conditions, as we mentioned before. The real space formulation of the self-consistency equation (18) is then given by

$$\hat{G}_0^{-1}(i!_n) = \hat{G}^c(i!_n) + \frac{1}{N_c} \sum_{K_c} \hat{t}_{DCA}(K_c) \hat{G}^c(i!_n) \quad (19)$$

where $[\hat{t}_{DCA}(K_c)]_{ij} = \frac{1}{N_c} \sum_{k_c} e^{ik_c} (e^{e_j}) t(k_c + K_c) = e^{ik} (e^{e_j}) t_{ij}(K_c)$ differs from the bare $\hat{t}(K)$ used in CDMFT in order to satisfy the cyclicity condition, i.e., the translational invariance. As in CDMFT, the solution requires an iterative solution of a cluster-impurity model determined self-consistently.

We now detail the implementation of the two approaches for the mean-field two-dimensional t - J model.

C. DCA for the saddle-point t - J model

In our analysis of the t - J model, the DCA cluster self-energy $\Sigma(k_c)$ consists of a normal term $\Sigma^N(k_c)$ and of an anomalous term $\Sigma^A(k_c)$, which are respectively the Fourier transform of γ_{ij} and γ_{ij}^A within the DCA cluster; explicitly, they are given by

$$\Sigma^N(k_c) = 2 \frac{DCA}{cl} (\cos k_{cx} + \cos k_{cy}); \quad (20)$$

$$\Sigma^A(k_c) = 2 \frac{DCA}{cl} (\cos k_{cx} - \cos k_{cy}); \quad (21)$$

Since our starting model is a mean-field model, these quantities are not independent; however, this deficiency is compensated by the possibility to solve exactly both the lattice and the cluster problems, even for large values of N_c .

The cluster parameters $\frac{DCA}{cl}$ and $\frac{DCA}{cl}$ are determined by the DCA self-consistency equations

$$\begin{aligned} \frac{DCA}{cl} &= \frac{3}{8} \int \frac{d^2 k}{(2\pi)^2} \text{hf}_k^y f_k^x i(\cos k_{cx} + \cos k_{cy}) \\ &= \frac{3}{8} \sum_{K_c} \int \frac{d^2 K}{(2\pi)^2} \frac{(K_c \cdot k_c)}{2E_{K_c}} \tanh \frac{E_{K_c}}{2} (\cos k_{cx} + \cos k_{cy}); \end{aligned} \quad (22)$$

$$\begin{aligned} \frac{DCA}{cl} &= \frac{3}{8} \int \frac{d^2 k}{(2\pi)^2} \text{hf}_k^x f_k^y i(\cos k_{cx} - \cos k_{cy}) \\ &= \frac{3}{8} \sum_{K_c} \int \frac{d^2 K}{(2\pi)^2} \frac{K_c}{2E_{K_c}} \tanh \frac{E_{K_c}}{2} (\cos k_{cx} - \cos k_{cy}); \end{aligned} \quad (23)$$

where $K_c \cdot k_c = 2t_e \frac{\cos(k_{cx} + K_x) + \cos(k_{cy} + K_y)}{(\frac{1}{L_c})^2 + \frac{1}{L_c^2}}$. In the second row of Eqs. (22){(23)} the integration over the entire Brillouin zone is divided into a sum over the cluster momenta and an integration over the reduced Brillouin zone, $\int \frac{d^2 k}{(2\pi)^2} = \frac{1}{L_c^2} \sum_{K_c} \int \frac{d^2 K}{(\frac{1}{L_c})^2}$.

It is important to note that these cluster quantities, used in the definition of the cluster self-energy, do not have an immediate physical meaning and thus they cannot be directly compared to the corresponding lattice quantities of Eqs. (10){(11)}. The physically relevant quantities are instead given by

$$\frac{DCA}{latt} = \frac{3}{8} \int \frac{d^2 k}{(2\pi)^2} \text{hf}_k^y f_k^x i(\cos k_x + \cos k_y); \quad (24)$$

$$\frac{DCA}{latt} = \frac{3}{8} \int \frac{d^2 k}{(2\pi)^2} \text{hf}_k^x f_k^y i(\cos k_x - \cos k_y); \quad (25)$$

where the expectation values must be evaluated using the self-consistent parameters $\frac{DCA}{cl}$ and $\frac{DCA}{cl}$, as in Eqs. (22){(23)}.

Finally, the DCA analogue of Eq. (12) gives the self-consistency equation for the chemical potential:

$$\begin{aligned} 1 - x &= 2 \int \frac{d^2 k}{(2\pi)^2} \text{hf}_k^y f_k^x i \\ &= 1 - \sum_{K_c} \int \frac{d^2 K}{(2\pi)^2} \frac{(K_c \cdot k_c)}{E_{K_c}} \tanh \frac{E_{K_c}}{2}; \end{aligned} \quad (26)$$

D. CDMFT for the saddle-point t - J model

Considering a square cluster C with $N_c = L_c \times L_c$ sites, we denote by $i = i_x + i_y = i_x + (i_y - 1)L_c$ the cluster site with coordinates (i_x, i_y) , where $i_x, i_y = 1; \dots; L_c$. The local cluster Hamiltonian is then obtained from the

lattice one by restricting all the site-index sums s to the cluster sites:

$$H_c = \sum_{i,j \in C} (t_{ij} + \hat{c}_{ij}) f_i^y f_j + \sum_{i \in C} f_i^y f_i + \sum_{i,j \in C} (\hat{c}_{ij} f_{i\#}^y f_{j\#}^y + h.c.); \quad (27)$$

where \hat{c} and \hat{t} are hermitian matrices and \hat{c} a symmetric matrix. Explicitly, their expressions read

$$t_{ij} = t_e \sum_{\mathbf{x}} (\delta_{j,i+\mathbf{x}} + \delta_{j,i-\mathbf{x}}); \quad (28)$$

$$\hat{c}_{ij} = \sum_{\mathbf{x}} \delta_{i,j+i\mathbf{x}} + \delta_{j,i-j\mathbf{x}}; \quad (29)$$

$$\hat{c}_{ij} = \sum_{\mathbf{x}} (\delta_{i,j+i\mathbf{x}} + \delta_{j,i-j\mathbf{x}}); \quad (30)$$

where $\mathbf{x} = x\hat{x} + y\hat{y}$ is a lattice displacement in the x or y direction, $j+i\mathbf{x} = j+i+1$ ($j-i-1$) in L_c , $j-i\mathbf{x} = j-i-1$ ($j+i+1$) in L_c and $j-i\mathbf{y} = j-i-L_c$. The self-consistent parameters \hat{c}_i and \hat{t}_i are formally given by Eqs. (5)-(6), where the expectation values must be evaluated using the cluster propagator \hat{D}_c , defined below.

In order to write this propagator in a compact form, we first introduce the Nambu spinor ψ^y ($f_{1\#}^y; \dots; f_{L_c\#}^y; f_{1\#}^y; \dots; f_{L_c\#}^y$), which contain all the $2L_c^2$ fermionic degrees of freedom within the cluster. With this notation,

$$\hat{D}_c(\mathbf{i}|\mathbf{n}) = \langle \psi^y(\mathbf{i})^\dagger \psi^y(\mathbf{n}) \rangle = \frac{\hat{G}_n(\mathbf{i}) \hat{F}_n^y(\mathbf{i})}{\hat{F}_n(\mathbf{i}) \hat{G}_n^T(\mathbf{i})}; \quad (31)$$

where $G_{ij} = \langle \psi_i^y \psi_j^y \rangle$ and $F_{ij} = \langle \psi_i^y \psi_{j\#}^y \rangle$ are, respectively, the normal and anomalous Green's functions. We can then express \hat{D}_c in terms of the cluster Hamiltonian parameters,

$$\hat{D}_c(\mathbf{i}|\mathbf{n}) = \sum_{\mathbf{x}} \frac{d^2 K}{2} \frac{h}{L_c} \hat{\psi}(\mathbf{i})^\dagger \hat{\psi}(\mathbf{n}) \hat{h}(\mathbf{K}); \quad (32)$$

$$\hat{h}(\mathbf{K}) = \frac{\hat{t}(\mathbf{K}) + \hat{c} \hat{t} \hat{c}}{(\hat{c}) \hat{t}(\mathbf{K}) + \hat{c} \hat{t} \hat{c}}; \quad (33)$$

where \hat{c} is the chemical potential times the unitary matrix, $\hat{t}(\mathbf{K})$ is the Fourier transform of the super-lattice hopping matrix $\hat{t}_{\mathbf{R},\mathbf{R}'}^0$, which, for $\mathbf{R} = \mathbf{R}' = \mathbf{j} = L_c$, connects the boundary sites of neighboring clusters:

$$t(\mathbf{K})_{ij} = t_{ij} - t_e \sum_{n=1}^{L_c} \exp(i\mathbf{K}_x L_c) \delta_{i,n} \delta_{j,(n-1)L_c+1} + \exp(i\mathbf{K}_x L_c) \delta_{j,n} \delta_{i,(n-1)L_c+1} + \exp(i\mathbf{K}_y L_c) \delta_{j,n} \delta_{i,L_c(L_c-1)+n} + \exp(-i\mathbf{K}_y L_c) \delta_{i,n} \delta_{j,L_c(L_c-1)+n}; \quad (34)$$

Introducing the unitary matrix $\hat{U}(\mathbf{K})$ which diagonalizes $\hat{h}(\mathbf{K})$,

$$\hat{U}(\mathbf{K}) \hat{h}(\mathbf{K}) \hat{U}^\dagger(\mathbf{K}) = \epsilon(\mathbf{K}); \quad (35)$$

we can write the cluster propagator as (the dependence of the matrices on \mathbf{K} is omitted to lighten the notation)

$$\hat{D}_c(\mathbf{i}|\mathbf{n}) = \sum_{\mathbf{I}} \frac{d^2 K}{2} \frac{h}{L_c} \hat{U}_{\mathbf{I}} \hat{U}_{\mathbf{J}}^\dagger \frac{1}{\epsilon(\mathbf{I})}; \quad (36)$$

where the index $\mathbf{I} = (i; j)$ denotes the $(-1)L_c^2 + 1$ component of a Nambu spinor ($i = 1, 2$).

It is now easy to get the self-consistency relations for the cluster parameters:

$$i_{i\mathbf{x}} = \frac{3}{8} \sum_{\mathbf{I}} \frac{d^2 K}{2} \frac{h}{L_c} \hat{U}_{\mathbf{I}} \hat{U}_{\mathbf{J}}^\dagger \hat{f}(\mathbf{I}); \quad i \in nL_c \quad (37)$$

$$i_{i\mathbf{y}} = \frac{3}{8} \sum_{\mathbf{I}} \frac{d^2 K}{2} \frac{h}{L_c} \hat{U}_{\mathbf{I}} \hat{U}_{\mathbf{J}}^\dagger \hat{f}(\mathbf{I}); \quad i \in nL_c \quad (38)$$

$$i_{i\mathbf{x}} = \frac{3}{8} \sum_{\mathbf{I}} \frac{d^2 K}{2} \frac{h}{L_c} \hat{U}_{\mathbf{I}} \hat{U}_{\mathbf{J}}^\dagger \hat{f}(\mathbf{I}); \quad i \in nL_c \quad (39)$$

$$i_{i\mathbf{y}} = \frac{3}{8} \sum_{\mathbf{I}} \frac{d^2 K}{2} \frac{h}{L_c} \hat{U}_{\mathbf{I}} \hat{U}_{\mathbf{J}}^\dagger \hat{f}(\mathbf{I}); \quad i \in nL_c \quad (40)$$

where $f(x) = (e^x + 1)^{-1}$ is the Fermi function.

The determination of the chemical potential as a function of the fermion density requires some more care. In fact, as we have seen in Eqs. (37)-(40) for \hat{c} and \hat{t} , the observables are generally site-dependent in CDMFT, and there is no unique procedure to extract lattice observables (translationally invariant) from cluster quantities. In general, for a local observable O_i , we can estimate its lattice counterpart with a weighted average

$$O_{\text{latt}} = \sum_{i \in C} w_i O_i; \quad (41)$$

where $\sum_{i \in C} w_i = 1$, and we have decided to investigate the two extreme cases of $w_i^{\text{at}} = 1/N_c$, and bulk value, $w_i^{\text{bulk}} = \delta_{i \in C}$, the latter case corresponding to

taking the value of the observable just in the center of the cluster¹⁸, represented by the site b . From the local fermion density

$$n_{bi} = 1 + \frac{\sum_{j=1}^Z \frac{d^2 K}{L_c^2} \hat{U}_{(1;i)}^2 \hat{U}_{(2;i)}^2}{\frac{2}{L_c}} = 1 \quad (42)$$

we can therefore extract an average density $n^{at} = 1/L_c^2 \sum_{i=1}^{L_c^2} n_{bi}$ and a bulk density $n^{bulk} = n_{bi}$, and we can adjust the chemical potential in order to satisfy either one of the two equations

$$n^{(at,bulk)} = 1 - x \quad (43)$$

The same argument would apply in extracting the lattice self-energy parameters, to be compared with those of Eqs. (10-11), from the corresponding cluster quantities. However, in considering the flat average case, we should note that \hat{c}_{ij} and \hat{c}_{ij}^\dagger are defined on bonds, so that for each direction their total number is $L_c(L_c - 1)$ instead of L_c^2 ; the averages will thus be given by

$$\hat{c}^{at} = \frac{1}{L_c(L_c - 1)} \sum_{i \in n L_c} \hat{c}_{i,x} \quad (44)$$

$$\hat{c}^{at} = \frac{1}{L_c(L_c - 1)} \sum_{i \in L_c(L_c - 1)} \hat{c}_{i,y} \quad (45)$$

$$\hat{c}^{at} = \frac{1}{L_c(L_c - 1)} \sum_{i \in n L_c} \hat{c}_{i,x} \quad (46)$$

$$\hat{c}^{at} = \frac{1}{L_c(L_c - 1)} \sum_{i \in L_c(L_c - 1)} \hat{c}_{i,y} \quad (47)$$

The bulk value estimate is instead straightforward and corresponds to the values of the parameters on the innermost bonds of the cluster.

II. RESULTS

A. Size dependence of observables

We start our analysis of DCA and CDMFT for the saddle-point t - J model by considering the behavior of three relevant observables as a function of the linear size of the cluster for square lattices of $L_c \times L_c$ sites. Throughout this section, energy scales are expressed in units of $J=4$ and $J=t=0.4$. In Fig. 1 we plot the superconducting order parameter for different values of doping $x = 0; 0.1$ and 0.2 . As discussed above, for CDMFT one has the alternative between "bulk" and "average" estimates. With respect to Δ , we have found that the average estimate is much less sensitive to the size of the system than the bulk one, the latter being instead rather unreliable, compared to the exact solution, up to large

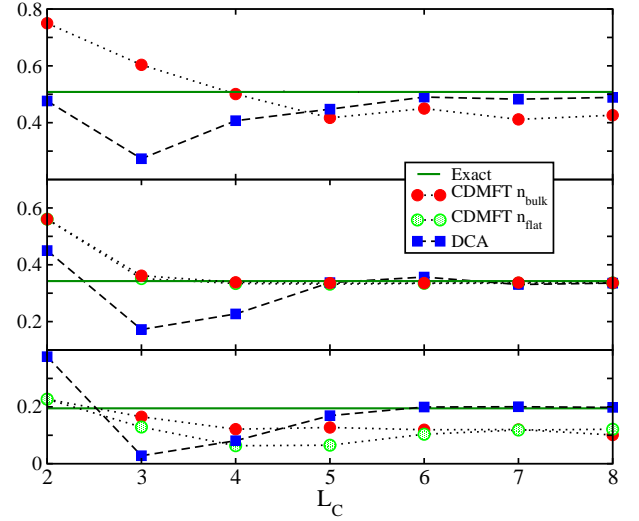


FIG. 1: (Color online). Normal parameter Δ as a function of the linear dimension L_c for square clusters and different cluster methods. Red dots are CDMFT with bulk density, green dots CDMFT with average density, blue squares DCA. The thermodynamic limit is marked by the thick green line. From top to bottom $x = 0; 0.1; 0.2$.

values of L_c . We will thus present, in each panel, only average estimates of Δ , while considering both the average and the bulk estimates of the electron density. The behavior of Δ as a function of the cluster size is completely non trivial and reveals important differences between the two methods. While DCA converges smoothly and faster from $L_c = 5$, it presents strong size-effects for smaller clusters: the $L_c = 2$ cluster overestimates Δ at large doping, while $L_c = 3$ and 4 produce a strongly underestimated value of Δ . This shows that momentum-space discretization is too strong to properly describe the spatial structure of the order parameter as long as the number of allowed momenta is small. On the other hand, while for $L_c = 2$ CDMFT overestimates Δ as well, the results obtained for small clusters are in general more reliable, with relatively small deviations from the exact solution and, most important, a smoother dependence on L_c . However, this method converges more slowly to the thermodynamic limit, in particular for larger dopings, where Δ is systematically underestimated. The comparison between different doping values shows indeed that CDMFT is quite inaccurate for $x = 0.2$, a doping value at which the hopping processes become more relevant, according to $t_e = xt$, making the system itinerant and consequently better described in momentum space than in real space. The bulk estimate of the density is typically found to provide a better agreement with the exact solution.

The same tendencies are present in the critical temperature (not shown), with a significantly enhanced overestimate of T_c compared to Δ in the $L_c = 2$ DCA cluster (we obtain $T_c = 1.53, 1.46$ and 1.30 for $x = 0; 0.1; 0.2$, while the exact results are $0.767, 0.601$ and 0.374). The sys-

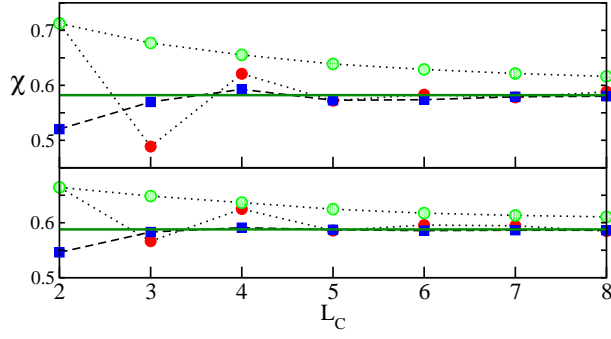


FIG. 2: (Color online) Normal parameter χ as a function of the linear dimension L_c for square clusters and different cluster methods. Red dots are CDMFT bulk values of χ , green dots CDMFT average values, blue squares DCA. The thermodynamic limit is marked by the thick green line. From top to bottom $x = 0.1; 0.2$.

tematic underestimate of T_c for large doping in CDMFT is also reflected in a smaller critical doping at which superconductivity disappears ($x_c \approx 0.25$ even for large clusters, as opposed to the thermodynamic limit $x_c \approx 0.35$).

We finally consider the normal parameter χ . Since this parameter coincides with χ_{CDMFT} at half-filling, due to the particle-hole symmetry, we focus only on $x = 0.1$ and 0.2 . Here, in agreement with previous studies in a one-dimensional model⁷, we find that in CDMFT the bulk estimate of the parameter is more accurate than the average one. Yet, CDMFT is less accurate than DCA for the cluster we studied, signaling that the exponential convergence of bulk estimates is established only for larger values of L_c .

The different behavior between the superconducting and the normal parameters underlines that the accuracy of the different approaches, for small clusters, depends crucially on the quantity under consideration. In particular, the d-wave superconducting order parameter suffers stronger size effects due to its peculiar structure in real-space, and, when the number of cluster sites becomes small, it is better represented by the CDMFT solution. On the other hand, the normal parameter, which is more isotropic, is better described by DCA, which favors homogeneous states (in the sense of states without peculiar patterns).

B. Doping dependence for small clusters

In this section we focus on the smallest clusters $L_c = 2; 3; 4; 5$, where we analyze in more details the doping dependence of the observables. This study is of particular interest because only small sizes can be handled in a full numerical solution of the Hubbard or t-J models using CDMFT and DCA approaches. For the sake of definiteness, in CDMFT we use the flat average estimate for both χ and Δ and the bulk estimate for the electron density.

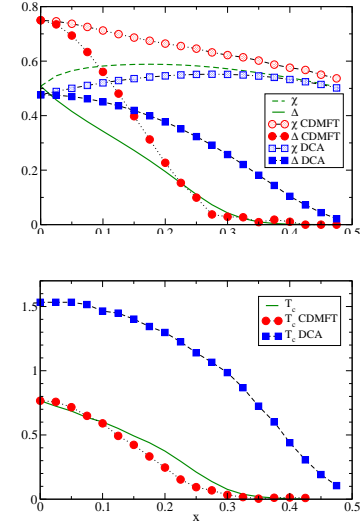


FIG. 3: (Color online) Doping dependence of χ and Δ (top) and of the critical temperature T_c (bottom) as a function of doping for a 2×2 cluster and different cluster methods. Filled symbols refer to χ , open symbols to Δ . Red dots are used for CDMFT, blue squares for DCA. The solid green line is the thermodynamic limit.

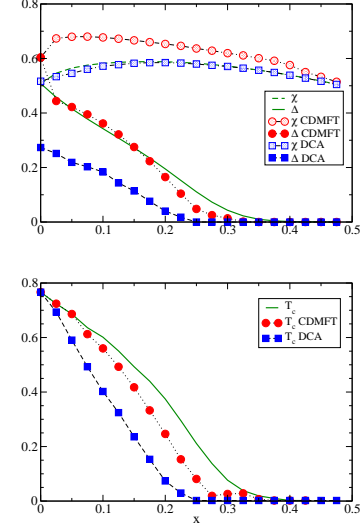


FIG. 4: (Color online) Same as Fig. 3 for 3×3 cluster.

We start with the $L_c = 2$ system, namely the so-called 2×2 plaquette. This is the smallest cluster that can host d-wave superconductivity, and its limited size makes it definitely the most popular system in CDMFT and DCA^{8,13}. From the results shown in Fig. 3 we find that both methods overestimate the d-wave order parameter, with stronger deviations at small x for CDMFT and for larger x in DCA. As far as the critical temperature is concerned, however, CDMFT turns out to reliably estimate the thermodynamic limit over almost the entire doping range, while DCA leads to a huge overestimate of T_c (a factor of 2 at half-filling, which increases as the

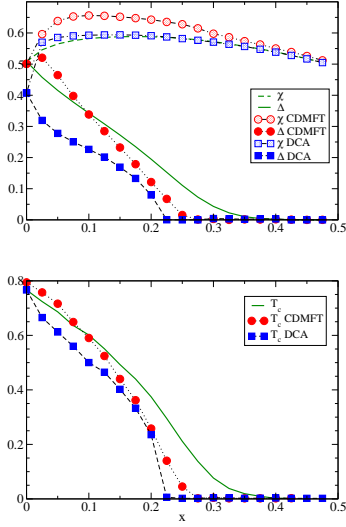


FIG. 5: (Color online) Same as Fig. 3 for 4 × 4 cluster.

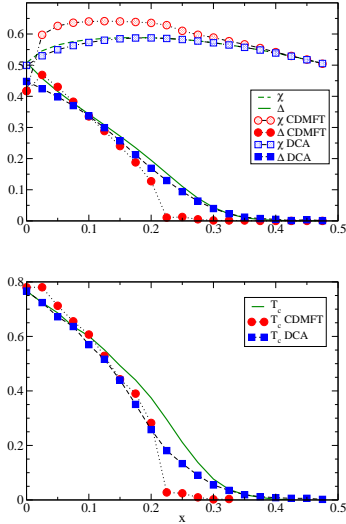


FIG. 6: (Color online) Same as Fig. 3 for 5 × 5 cluster.

doping grows). These results suggest that the geometrical constraints imposed by the 2 × 2 cluster have extremely strong effects on the d-wave phase, making this kind of cluster hardly useful for a quantitative estimate. Nonetheless, the simplicity of this cluster makes it a simple instrument to analyze the essential physics of two-dimensional correlated models.

As soon as we increase the size of the cluster to $L_c = 3$, CDMFT experiences a substantial improvement. Both Δ and T_c are indeed reasonably close to the exact solution, except for a moderate bifurcation of T_c for large doping. Conversely, DCA strongly underestimates both quantities. It should be noted that odd values of L_c explicitly break the particle-hole symmetry which holds at half-filling in the original model, since the (π, π) point of the Brillouin zone is not included among the cluster momenta: this is the reason why Δ and T_c are not equal for

$x = 0$. The success of CDMFT for this small cluster has a twofold interest: on one hand it is a promising direction for full numerical solutions of the Hubbard model, since the size of this cluster is reasonably small to allow for a reasonably accurate numerical accuracy; on the other hand it suggests us that, from a geometrical point of view, it is important to have at least two independent local amplitudes for the field (the symmetry group of square clusters allows two independent bonds for $L_c = 3$, in CDMFT, while in the corresponding DCA cluster there is only one independent (k_c)).

For the $L_c = 4$ cluster the two approaches give essentially analogous results, and none of them is particularly interesting. This underlines the fact that, for such small values, the precise shape of the cluster matters more than the total number of sites, and that the inclusion of the (π, π) point improves the DCA results, even if not by a large amount.

Interestingly, at $L_c = 5$ DCA becomes substantially more accurate than CDMFT. This confirms that DCA enters the asymptotic regime more rapidly than CDMFT, for which the finite-size effects survive to larger clusters, as we anticipated in the previous section.

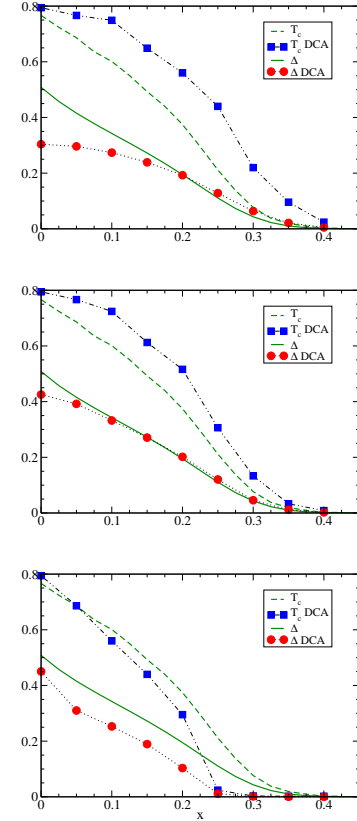


FIG. 7: (Color online) Doping dependence of Δ and T_c in DCA for tilted clusters ($N_c = 8; 12; 16$ from top to bottom).

C . Tilted Clusters

As we mentioned above, when dealing with very small clusters the DCA solution may suffer of severe size effects, associated to the presence or absence of characteristic cluster momenta, of special relevance, such as $(\pi; 0)$, $(0; \pi)$. A potential solution for this kind of sensitivity to the specific size and shape of the cluster is the use of specific "tilted" lattices, as shown in Ref.15,19. These clusters are compatible with the space group of the lattice, and at the same time are expected to display less important size effects than the standard square systems. Our analysis shows that, unfortunately, the improvement brought by the tilted lattices is not substantial. In Fig. 7 we display DCA results for $N_c = 8; 12; 16$ sites in tilted lattices, and we found that an accuracy comparable to that of the 5×5 square cluster is obtained only for $N_c = 20$, i.e., with almost the same number of sites.

D . More specific lattices

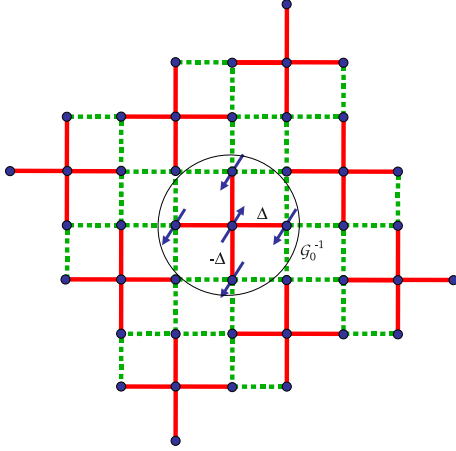


FIG. 8: (Color online) Cross cluster and its embedding in the 2-d lattice.

One of the outcomes of our analysis so far is that, as long as the size of the cluster is not sufficiently large, the accuracy of the results is dominated by geometrical factors. Therefore it is interesting to consider small specific clusters, whose size can be accessible to full numerical solutions, and that can minimize the geometrical frustration (or enhancement) of the d-wave superconducting state.

To this aim we studied the "cross" cluster, shown in Fig. 8 together with its embedding in the two-dimensional space, and small rectangular lattices. The star geometry can be considered as a good choice, since it can fit a d-wave "cross" of nearest-neighbor bonds. We find that the two approaches perform quite differently for this lattice. While CDMFT does not provide particularly accurate results, DCA reproduces remarkably well

the exact solution for both the order parameter and the critical temperature T_c . Interestingly, the accuracy in the superconducting parameters is not accompanied by an equally good description of the normal self-energy

(results are not shown). The accuracy of DCA is associated to the particular values of the cluster momenta $K_c = (0; 0)$, $(\pi; \pi)$ and $(\pi; 0)$, $(0; \pi)$, which exclude the special symmetry points $(0; \pi)$ and $(\pi; 0)$, but are at the same time close enough to the anti-nodal points to properly treat the superconducting order parameter. On the other hand, the momenta which are most important to describe are not included, leading to a worse estimate.

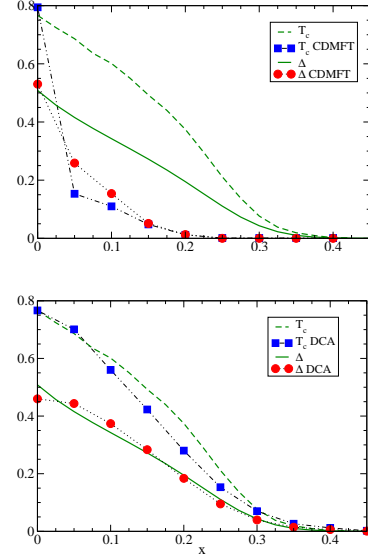


FIG. 9: (Color online) Doping dependence of Δ and T_c for the cross cluster ($N_c = 5$). Top panel is CDMFT, bottom panel DCA.

As far as CDMFT is concerned, much closer agreement with the thermodynamic limit is reached, as shown in Fig. 10, using (small) rectangular lattices. Already the 2×3 rectangle provides quite accurate results over the entire range of dopings, and the 3×4 one shows a remarkable agreement with the thermodynamic limit. An explanation for the success of such clusters could be found in the relatively large number of independent bonds compared to their total number, which is a consequence of the lower symmetry of the cluster space group. DCA on these rectangular lattices does not lead to particularly accurate results. Essentially the results (not shown) can be seen as a slight improvement on the corresponding square lattice (the largest square lattice contained in the rectangle), as far as T_c is concerned.

We have thus identified at least two relatively small lattices which provide accurate results and that can be reasonably approached using a full numerical solution of CDMFT or DCA for the quantum Hubbard or t-J models, namely the 5-site cross for DCA and the 6-site rect-

- ⁶ M . Pottho , Phys. Rev. B 70, 245110 (2004); A . N . Rubtsov, M . I . Katsnelson, and A . I . Lichtenstein, Phys. Rev. B 77, 033101 (2008); A . I . Lichtenstein and M . I . Katsnelson, Phys. Rev. B 62, R 9283 (2000); D . Snchal, P . L . Lavertu, M . A . M arois, and A . M . S . Tremblay, Phys. Rev. Lett. 94, 156404 (2005); S . Okamoto, A . J . M illis, H . Monien, and A . Fuhrmann, Phys. Rev. B 68, 195121 (2003)
- ⁷ See, G . Biroli and G . Kotliar, Phys. Rev. B 65 155112 (2002), comment by K . A ryanpour, Th . A . Maier, and M . Jarrell and reply.
- ⁸ Th . A . Maier, M . Jarrell, A . Macridin, and C . Slezak, Phys. Rev. Lett. 92, 027005 (2004); M . C ivelli, M . Capone, A . Georges, K . Haule, O . Parcollet, T . D . Stanescu, and G . Kotliar, Phys. Rev. Lett. 100, 046402 (2008); S . S . Kancharla, B . Kyung, D . Snchal, M . C ivelli, M . Capone, G . Kotliar, and A . M . S . Tremblay, Phys. Rev. B 77, 184516 (2008); K . Haule and G . Kotliar, Phys. Rev. B 76, 104509 (2007)
- ⁹ J . E . Hirsch and R . M . Fye, Phys. Rev. Lett. 56, 2521 (1986)
- ¹⁰ A . N . Rubtsov, V . V . Savkin, and A . I . Lichtenstein, Phys. Rev. B 72, 035122 (2005); P . W emer, A . Comanac, L . de' Medici, M . Troyer, A . J . M illis, Phys. Rev. Lett. 97, 076405 (2006)
- ¹¹ M . Carrel and W . K rauth, Phys. Rev. Lett. 72, 1545 (1994); M . Capone, L . de' Medici, A . Georges, Phys. Rev. B 76, 245116 (2007)
- ¹² R . Bulla, Phys. Rev. Lett. 83, 136 (1999)
- ¹³ M . C ivelli, M . Capone, S . S . Kancharla, O . Parcollet, and G . Kotliar Phys. Rev. Lett. 95, 106402 (2005); A . Macridin, M . Jarrell, Th . Maier, P . R . C . Kent, E . D 'A zevedo, Phys. Rev. Lett. 97, 036401 (2006); Th . A . Maier, Th . P ruschke, and M . Jarrell, Phys. Rev. B 66, 075102 (2002); B . Kyung, S . S . Kancharla, D . Snchal, A . M . S . Tremblay, M . C ivelli, and G . Kotliar Phys. Rev. B 73, 165114 (2006)
- ¹⁴ M . Jarrell, Th . Maier, C . H uscroft, and S . M oukouri, Phys. Rev. B 64, 195130 (2001)
- ¹⁵ T . A . Maier, M . Jarrell, T . C . Schulthess, P . R . C . Kent and J . B . W hite, Phys. Rev. Lett. 95, 237001 (2005)
- ¹⁶ G . Kotliar and J . Liu, Phys. Rev. B 38, 5142 (1988)
- ¹⁷ I . A eck and J . B . M arston, Phys. Rev. B 37, 3774 (1998).
- ¹⁸ For even values of L_c the center of the cluster is not represented by a single site, but instead by a 4{site plaquette; this sites are however equivalent to each other, since they are connected by the cluster symmetry group.
- ¹⁹ D . D . Betts, H . Q . Lin and J . S . F lynn, Can. J. Phys. 77, 353 (1999)